High Selectivity Dual-Band Bandpass Filter with Flexible Passband Frequencies and Bandwidths

Yalin Ma[1,2], Wenquan Che[1], Wenjie Feng[1], and Jianxin Chen[3]

[1]Department of Communication Engineering, Nanjing University of Science and Technology, Nanjing 210094, China

[2]Faculty of Mathematics and Physics, Huaiyin Institute of Technology, Huai'an 223003, China

[3]School of Electronics and Information, Nantong University, Nantong 226019, China

yeeren_che @163.com

Abstract ─ A short-ended resonator with open stub loaded is presented in this paper. Resonance property is analyzed based on the transmission line theory. Analysis reveals that the odd/even-mode resonance frequency of the proposed resonator can be conveniently controlled. To realize two controllable bandwidths, two different coupling paths are introduced in the filter design. Furthermore, to improve the filter selectivity, the source-load coupling is adopted to create four transmission zeros (TZs) near the edges of the two passbands. Thus, a dual-band bandpass filter (BPF) with high selectivity can be achieved. One filter with two passband frequencies at 1.01 GHz and 2.4 GHz is designed and fabricated to provide an experimental verification on the design method.

Index Terms ─ Bandwidth, dual-band bandpass filter, passband frequency, and transmission zero.

I. INTRODUCTION

With the increasing demands for multi-band application in modern wireless system, it is popular for researches on the design of multi-band filters recently [1-9], especially dual-band filters [4-9]. In the past years, three design methods are introduced. The first one is to combine two sets of resonators with common input and output ports [3]. The passband frequencies can be independently controlled by using the proper configuration. However, the control of passband bandwidths is not discussed. The second one is to use stepped-impedance resonators (SIR) [5-7] and shorted-end resonators [8] to create two passbands. Although the passband frequencies can be tuned to the desire values, it is difficult to control the bandwidths. The last one is to use two coupling paths to realize the dual-band filters with controllable bandwidths, and the passband frequencies can be controlled by impedance ratio [9]. However, it is not convenient to realize the control of passband frequencies and bandwidth. To solve this problem, dual-band inverters are utilized to obtain the desired frequency and bandwidth at each passband [10].

In this paper, a short-ended resonator with open stub loaded for designing a dual-band filter with the flexible passband frequencies and bandwidths is proposed. The passband frequencies can be flexibly controlled by selecting the proper structure parameters of the open stubs and shorted ends. The bandwidths of the two passbands can be conveniently controlled by two coupling paths. By properly controlling the coupling coefficients of the coupling paths, the bandwidths can be controlled. As a result, both the passband frequencies and bandwidths can be easily adjusted. In addition, source-load coupling scheme (the third coupling path) is also introduced to create two TZs near the edges of each passband, resulting in high skirt selectivity.

Submitted On: Dec. 12, 2012
Accepted On: Feb. 6, 2013

II. ANALYSIS AND DESIGN OF PROPOSED BPF

Figure 1 shows the configuration of the proposed microstrip BPF, which is composed of two resonators and two feed lines. The resonator is constructed by a short-ended resonator with an open-circuited stub at the center. The resonators are folded to reduce the circuit area. As can be seen from Fig. 1, there are two coupling paths between the two resonators, i.e., *Path 1* and *Path 2*. *Path 1* indicates the coupling near the ends of the short-ended resonators, while *Path 2* is the coupling between the two open stubs. Furthermore, the source-load coupling between the two feed lines does exist, causing improvement of the selectivity, which is donated as *Path 3* in Fig. 1.

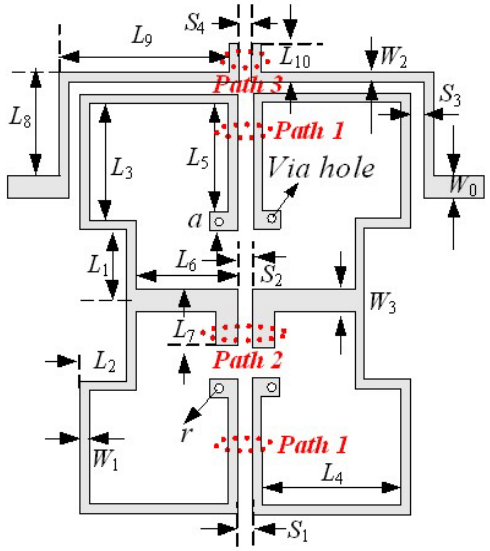

Fig. 1. Configuration of the proposed BPF.

A. Control of passband frequencies

Figure 2 (a) shows the structure of the proposed resonator, which is composed of short-circuited resonator at both ends and an open-circuited stub at the midpoint. If the odd-mode excitation is applied to Feed 1 and 2, there is a voltage null at the symmetric plane (*T*-*T*) of the resonator. Therefore, the equivalent circuit can be attained, as shown in Fig. 2 (b). The input admittance for the odd mode is given by,

$$Y_{ino} = -j\frac{Y}{\tan\theta_1} - j\frac{Y}{\tan\theta_2}. \quad (1)$$

Where $\theta_1 = \beta l_1$, $\theta_2 = \beta l_2$, β is the propagation constant of the fundamental frequency. Y donates the characteristic admittance of the transmission line with shorted ends. Thus, the resonance condition is that the imaginary part of Y_{ino} is equal to zero, the odd-mode fundamental resonance frequencies can be deduced as,

$$f_o = \frac{nc}{2(l_1+l_2)\sqrt{\varepsilon_e}}. \quad (2)$$

Where $l = 2\,(l_1 + l_2)$, n = 1, 2, 3 …, c is the speed of light in free space, and ε_e denotes the effective dielectric constant.

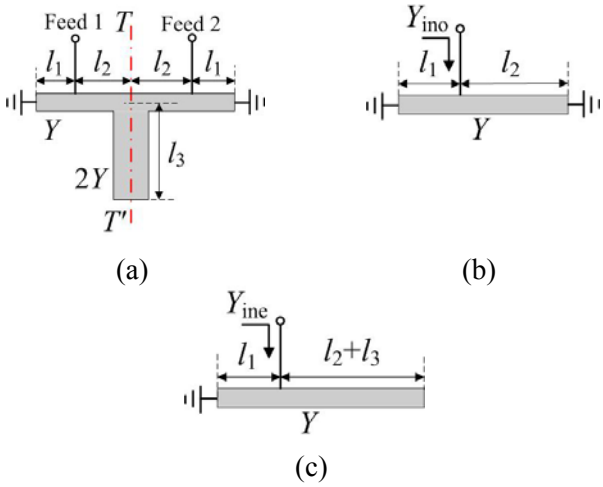

Fig. 2. (a) Structure of the proposed resonator, (b) equivalent circuit of the odd mode, and (c) equivalent circuit of the even mode.

If the even-mode excitation is applied to Feed 1 and 2 shown in Fig. 2 (a), there is no current flowing through the symmetric plane (*T*-*T*) of the transmission line. Therefore, the equivalent circuit can be attained by symmetrically bisecting the resonator, as shown in Fig. 2 (c). The input admittance for the even mode is expressed as

$$Y_{ine} = -j\frac{Y}{\tan\theta_1} + jY\frac{\tan\theta_2 + \tan\theta_3}{1-\tan\theta_2\tan\theta_3}, \quad (3)$$

where $\theta_3 = \beta l_3$. The resulted even-mode fundamental resonance frequencies can be attained as follow,

$$f_e = \frac{(2n-1)c}{2(l+2l_3)\sqrt{\varepsilon_e}}. \quad (4)$$

A full-wave EM eigenmode simulation is also used to study the resonance properties of the proposed resonator. The electric field pattern at the odd-mode resonance frequency is illustrated in Fig. 3 (a). It can be seen that the minimum fields are near the region of via hoes and stub. Furthermore, the field exhibits an anti-symmetric property along the symmetric line T-T'. As for the electric field pattern at the even-mode resonance frequency that is illustrated in Fig. 3 (b), the minimum fields are only near the region of via holes together with a symmetric property along the symmetric line T-T'.

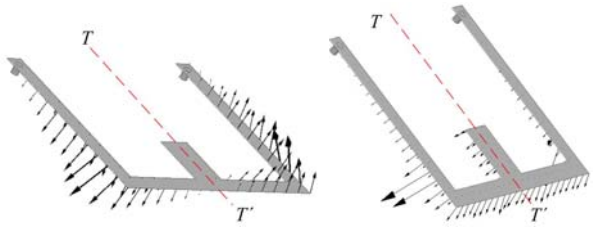

(a) (b)

Fig. 3. Simulated electric field patterns for the proposed resonator for (a) odd mode and (b) even mode.

It can be observed from equations (2) and (4) and Fig. 3 that the relation $f_o > 2f_e$ can be attained. Furthermore, the odd-mode resonance frequencies are determined by the length of the shorted ends and the even-mode resonance frequencies are determined by the lengths of the shorted ends and open stub, i.e., changing the even-mode resonance frequencies may not affect the odd-mode resonance frequencies. With this property, dual-band filters with the flexible passband frequencies can be designed. Using the configuration in Fig. 1, the passband frequencies can be conveniently controlled. For validation, full-wave simulation is carried out using HFSS. Other parameters of the filter in Fig. 1 are kept fixed and only the lengths of L_4 and L_7 are changed, respectively. The simulated responses of the passband frequencies versus the lengths of L_4 and L_7 are shown in Fig. 4 (a) and 4 (b), respectively. It can be seen that both passband frequencies are shifted down by changing the length of L_4. Moreover, the lower passband frequency (f_L) is shifted down by changing the length of L_7, while the upper one (f_H) is preserved. Besides, f_H is larger than twice of f_L.

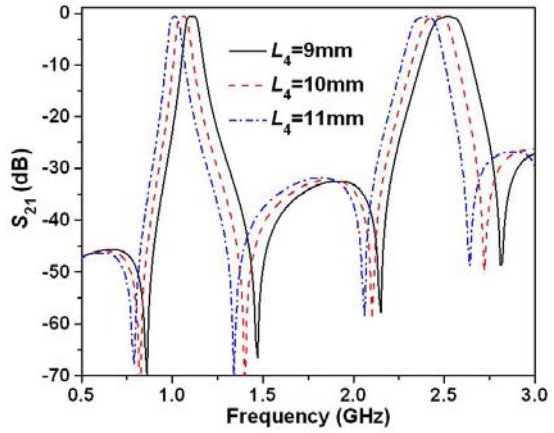

(a)

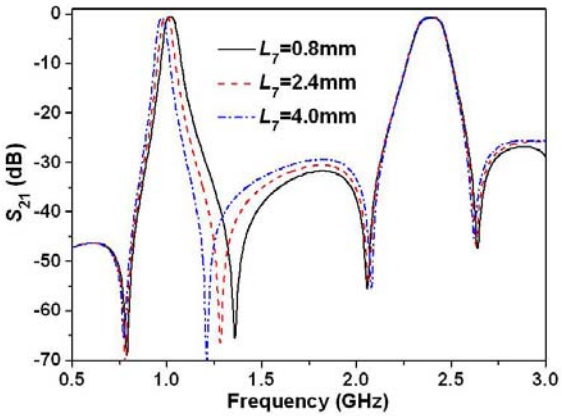

(b)

Fig. 4. Simulated responses of the passband frequencies versus length of (a) L_4 and (b) L_7.

B. Control of passband bandwidths

The coupling paths of the proposed filter are shown in Fig. 1. The coupling scheme for the two

bands is shown in Fig. 5. According to the above discussions, the lower passband is decided by the shorted ends and open stubs while the upper passband is only decided by the shorted ends. Thus, the two passband bandwidths are affected by the first two coupling paths and the upper passband bandwidth is only determined by the first coupling path. To determine the coupling bandwidths, two feed lines are weakly coupled to the two resonators, respectively. From the S_{21} plotted in Fig. 6, it is observed that the odd and even resonance modes are split into four transmission poles termed as f_{o1}, f_{o2}, f_{e1}, and f_{e2}. The coupling coefficients and absolute bandwidths (ABWs) for the two passbands are mainly determined by the coupling gaps and can be calculated as,

$$\begin{aligned} |k_L| &= \left|k_{path1L} + k_{path2L}\right| = \left|k_{eL} + k_{mL}\right| \\ &= x(S_1, S_2) = \left(f_{e2}^2 - f_{e1}^2\right) \Big/ \left(f_{e1}^2 + f_{e2}^2\right) \end{aligned} \tag{5}$$

$$\begin{aligned} |k_H| &= \left|k_{path1H}\right| = \left|k_{mH}\right| = x(S_1) \\ &= \left(f_{o2}^2 - f_{o1}^2\right) \Big/ \left(f_{o1}^2 + f_{o2}^2\right), \end{aligned} \tag{6}$$

$$\Delta_L = y(S_1, S_2) = f_{e2} - f_{e1}, \tag{7}$$

$$\Delta_H = y(S_1) = f_{o2} - f_{o1}. \tag{8}$$

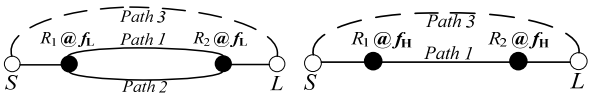

(a) (b)

Fig. 5. Coupling mechanism, (a) for the lower resonance frequency and (b) for the upper resonance frequency.

It can be seen from equations (6) and (8) that the coupling coefficients and ABWs of the upper passband ($|k_H|$ and Δ_H) are only affected by the gap of S_1 (*Path 1*), which can be confirmed from Figs. 7 and 8. It can be observed from equations (5) and (7) that $|k_L|$ and Δ_L are affected by the gaps of S_1 and S_2 (*Path 1* and *Path 2*). As discussed in [11], *Path 1* is the magnetic coupling and *Path 2* is the electric coupling, so $k_{path1L} = k_{mL} < 0$ and $k_{path2L} = k_{eL} > 0$ can be achieved. Furthermore, $|k_{path1L}|$ (= $|k_{mL}|$) is decreased with the increase of S_1 while k_{path2L} (= $k_{eL} > 0$) keeps unchanged. In addition, $|k_L|$ is decreased with the increase of S_1, as shown in Fig. 7 (a). According to equation (5), $|k_{path1L}| = |k_{mL}| > |k_{path2L}| = |k_{eL}|$ can be achieved. Thus, $|k_L|$ and Δ_L are increased with the increase of S_2, which can be seen from Figs. 7 (b) and 8 (b).

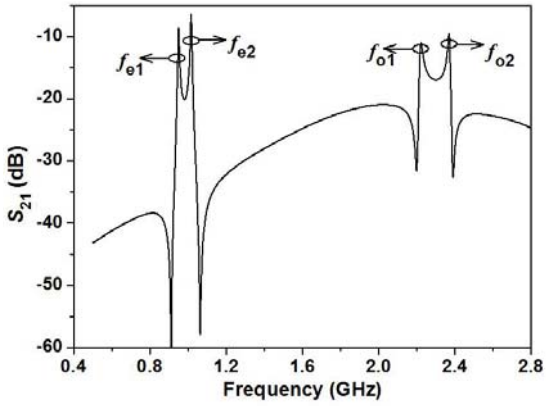

Fig. 6. Resonance frequency of the proposed BPF for S_3 = 1.0 mm.

Besides the coupling coefficients, the external quality factors (Q_es) also affects the bandwidths. In this design, Q_es for the two passbands may be determined by k' and L_8. Here k' (=(Z_E-Z_O) / (Z_E+Z_O)) is the coupling coefficient between the feeder and the resonator, and Z_E, Z_O are the even and odd characteristic impedances. The simulated Q_es for the two passbands against k' and L_8 are shown in Fig. 9. Here, Q_{e1} and Q_{e2} are the external quality factors for the lower and upper passbands, respectively. It can be observed that Q_es for the two passbands are increased with the increase of k' and slightly affected by L_8. Hence, Q_es for the two bandwidths can be tuned to the desired values by adjusting k' within a certain range. Therefore,

there are sufficient degrees of freedom to control the bandwidths at the two passbands.

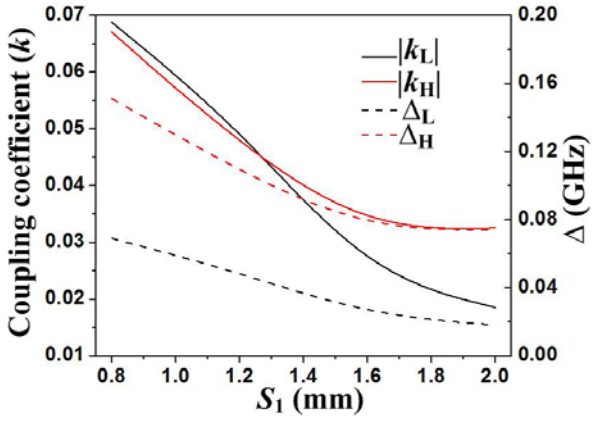

(a)

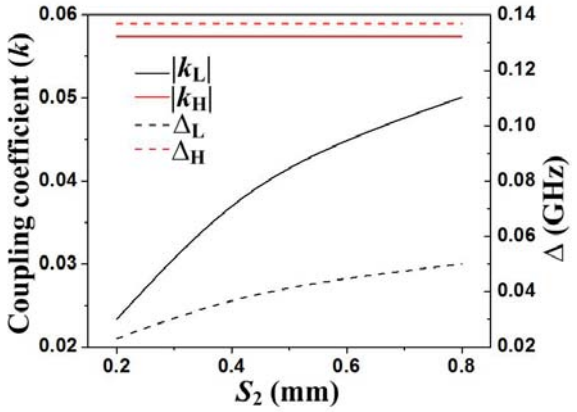

(b)

Fig. 7. k and Δ versus gap of (a) S_1 and (b) S_2.

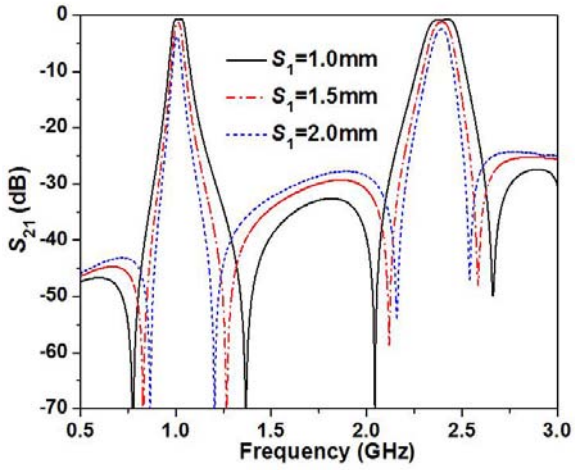

(a)

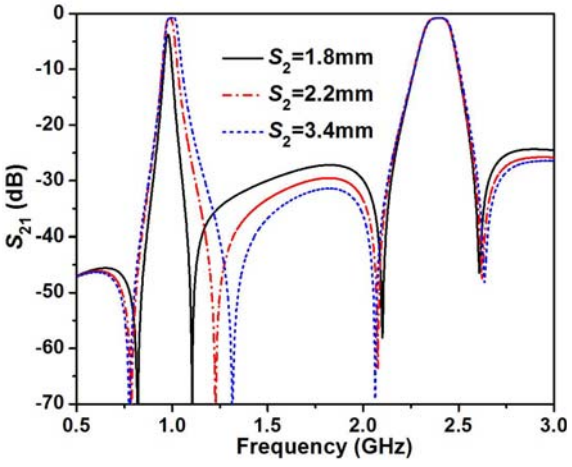

(b)

Fig. 8. Simulated responses of the passband bandwidths versus gap of (a) S_1 and (b) S_2.

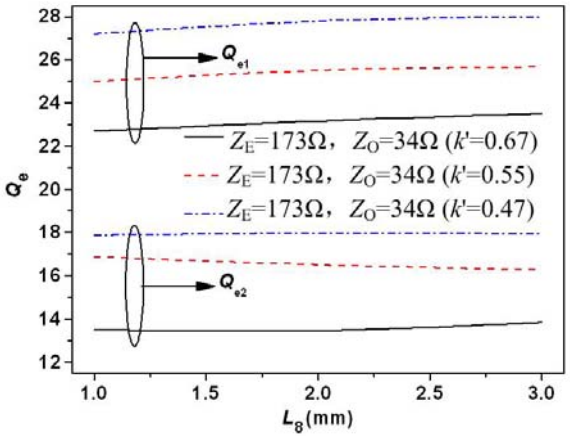

Fig. 9. Simulated Q_es for the passbands against k' and L_8.

C. Design methodology

To design the proposed filter, the first step is to obtain desirable passband frequencies. As stated above, the open stub will not affect f_H. Therefore, we first tune f_H to the desirable value by changing the length of the short-circuited line. After that, the open-stub length is adjusted to obtain desirable f_L without affecting f_H.

The second step is to obtain the required bandwidths at f_L and f_H. As stated previously, the coupling *Path 2* has no impact on the upper

passband. Hence, we first meet the requirement of $|k_H|$ and Δ_H by changing the dimensions of *Path 1* and then obtain desirable $|k_L|$ and Δ_L by altering the dimensions of *Path 2*. As for the Q_es, we can tune k' to control it. Finally, a fine tuning is performed to fulfill the requirements of both passbands.

III. MEASURED RESULTS AND DISCUSSIONS

To demonstrate our design, one prototype of the proposed dual-band BPF is implemented on a substrate with ε_r = 3.38 and h = 0.813 mm. The dimensions are determined as follows: W_0 = 1.9 mm, W_1 = 0.4 mm, W_2 = 0.4 mm, W_3 = 0.8 mm, S_1 = 1.1 mm, S_2 = 0.9 mm, S_3 = 0.15 mm, S_4 = 0.4 mm, L_1 = 5.7 mm, L_2 = 3.5 mm, L_3 = 10.1 mm, L_4 = 11.0 mm, L_5 = 9.2 mm, L_6 = 8.0 mm, L_7 = 1.2 mm, L_8 = 9.2 mm, L_9 = 12.3 mm, L_{10} = 1.1 mm, r = 0.3 mm, and a = 1.4 mm. Figure 10 shows the photograph and measured results of the proposed dual-band filter. The measured passband frequencies of the two passbands are 1.01 GHz and 2.4 GHz, and the measured minimum insertion loss (IL) of the two passbands are 0.9 dB and 1.0 dB, with the 3 dB fractional bandwidth (FBW) of 5.92 % and 5.86 %. Inside the passbands, the return loss is greater than 15.5 dB. Four TZs are created by the source-load coupling at 0.79 GHz, 1.34 GHz, 2.06 GHz, and 2.64 GHz near the edges of the two passbands, improving the selectivity of the filter. Furthermore, the rejection level between adjacent bands is better than -30 dB. Besides, a wide upper stopband with a good suppression of greater than 15 dB from 2.56 GHz to 4.8 GHz has been realized. Table 1 summarizes the comparisons of the proposed filter with previous reports. The proposed dual-band BPF has the advantages of compact size, wide upper stopband, high selectivity, and independent control of center frequencies and bandwidths.

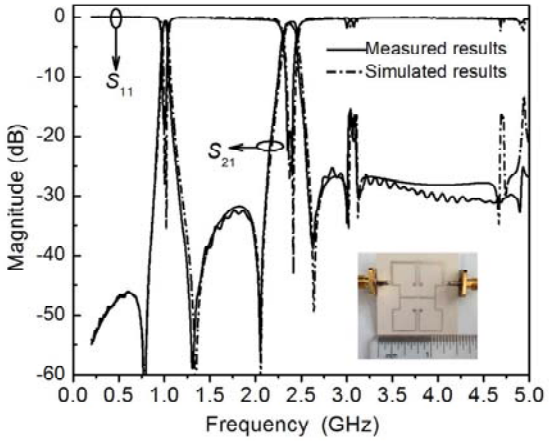

Fig. 10. Results and photograph of the proposed dual-band BPF.

Table 1: Comparisons of dual-band BPFs.

Ref.	Effective circuit size	TZs	IL (dB)	3-dB FBW (%)
[4]	$0.10\lambda_0\times0.25\lambda_0$	5	0.85/0.9	10/9.3
[5]	$0.21\lambda_0\times0.25\lambda_0$	1	1.8/2.9	7.0/4.0
[6]	$0.14\lambda_0\times0.14\lambda_0$	2	0.8/1.0	54/20
[7]	$0.25\lambda_0\times0.25\lambda_0$	6	1.58/1.54	2.0/3.3
[8]	$0.29\lambda_0\times0.37\lambda_0$	4	1.8/ 1.6	7.3/ 9.8
[9]	$0.22\lambda_0\times0.21\lambda_0$	2	1.46/1.16	5.5/4.5
Proposed filter	$0.14\lambda_0\times0.19\lambda_0$	6	0.9/1.0	5.9/5.8

λ_0 is the guided wavelength of the lower passband.

IV. CONCLUSION

This paper has proposed a resonator for the design of a dual-band BPF. The passband frequencies and bandwidths of the proposed filter can be conveniently controlled by adjusting the corresponding resonator structure parameters and the coupling coefficients properly. Four TZs near the edges of the passbands can be realized by source-load coupling. The filter has the advantages of flexible passband frequencies and bandwidths, compact size, high selectivity, and wide upper stopband. With all these properties, the proposed filter is applicable for dual-band wireless communication systems.

ACKNOWLEDGEMENT

This work was supported by the Natural Science Foundation of China (60971013), the 2009 Innovative Graduate Projects of Jiangsu Province and the Program for New Century Excellent Talents in University (NCET-11-0993).

REFERENCES

[1] S. Gao, S. Xiao, and J. L. Li, "Compact ultra-wideband (UWB) bandpass filter with dual notched bands," *Appl. Comp. Electro. Society Journal*, vol. 27, no. 10, pp. 795-800, Oct. 2012.

[2] C. Liu, Y. Li, and J. Zhang, "A novel UWB filter with WLAN and RFID stop-band rejection characteristic using tri-stage radial loaded stub resonators," *Appl. Comp. Electro. Society Journal*, vol. 27, no. 9, pp. 749-758, Sep. 2012.

[3] A. Eroglu and R. Smith, "Triple band bandpass filter design and implementation using SIRs," *26th Annual Review of Progress in Appl. Comp. Electro.*, Tampere, Finland, pp. 862-865, Apr. 2010.

[4] G. L. Dai, Y. X. Guo, and M. -Y. Xia, "Dual-band bandpass filter using parallel short-ended feed scheme," *IEEE Microw. Wireless Compon. Lett.*, vol. 20, no. 6, pp. 325–327, June 2010.

[5] S. Sun and L. Zhu, "Compact dual-band microstrip bandpass filter without external feeds," *IEEE Microw. Wireless Compon. Lett.*, vol. 15, no. 10, pp. 644-646, Oct. 2005.

[6] K. S. Chin and J. -H. Yeh, "Dual-wideband bandpass filter using short-circuited stepped-impedance resonators," *IEEE Microw. Wireless Compon. Lett.*, vol. 19, no. 3, pp. 155-157, Mar. 2009.

[7] C. W. Tang and P. H. Wu, "Design of a planar dual-band bandpass filter," *IEEE Microw. Wireless Compon. Lett.*, vol. 21, no. 7, pp. 362-364, July 2011.

[8] L. Gao and X. Y. Zhang, "Novel dual-band bandpass filters using stub-loaded short-ended resonators," *Microw. Opt. Tech. Lett.*, vol. 54, no. 12, pp. 2771-2774, Dec. 2012.

[9] X. Y. Zhang, C. H. Chan, Q. Xue, and B. J. Hu, "Dual-band bandpass filter with controllable bandwidths using two coupling paths," *IEEE Microw. Wireless Compon. Lett.*, vol. 20, no. 11, pp. 616-618, Nov. 2010.

[10] H. M. Lee and C. M. Tsai, "Dual-band filter design with flexible passband frequency and bandwidth selections," *IEEE Trans. Microwave Theory Tech.*, vol. 55, no.5, pp. 1002-1009, May 2007.

[11] J. S. Hong and M. J. Lancaster, *Microwave Filter for RF/Microwave Application*, New York: Wiley, 2001.

Yalin Ma received the M. Sc. degree from UESTC, Chengdu, China, in 2006. He is currently working toward the Ph.D. degree in Electromagnetic Field and Microwave Technology in NJUST. His research interest is the design of tunable circuits, differential network, etc.

Wenquan Che received the M.Sc. degree from NUST, Nanjing, China, in 1995, and the Ph.D. degree from the City University of Hong Kong (CITYU), Kowloon, Hong Kong, in 2003. She is currently a Professor with NUST, Nanjing, China. Her research interests include electromagnetic computation, planar/coplanar circuits and subsystems in RF/microwave frequency, microwave monolithic integrated circuits (MMICs) and medical application of microwave technology.

Wenjie Feng received the M.Sc. degree from NUST, Nanjing, China, in 2010, and is currently working toward the Ph.D. degree in Electromagnetic Field and Microwave Technology in NJUST. His research interests include ultra-wideband (UWB) circuits and technologies, etc.

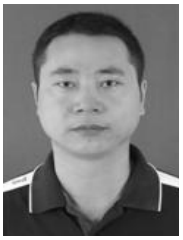

Jianxin Chen received the M.Sc. degree from UESTC, Chengdu, China, in 2004, and the Ph.D. degree from CITYU, Kowloon, Hong Kong, in 2008. He is currently a Professor with Nantong University, Jiangsu Province, China. His research interests include RF/microwave active and passive circuit designs.